The Astrophysical Journal, 658:1328–1339, 2007 April 1

LOOKING FOR GIANT EARTHS IN THE HD 209458 SYSTEM: A SEARCH FOR TRANSITS IN *MOST*[1] SPACE-BASED PHOTOMETRY

Bryce Croll,[2] Jaymie M. Matthews,[2] Jason F. Rowe,[2] Rainer Kuschnig,[2] Andrew Walker,[3]
Brett Gladman,[2] Dimitar Sasselov,[4] Chris Cameron,[2] Gordon A. H. Walker,[5]
Douglas N. C. Lin,[6] David B. Guenther,[7] Anthony F. J. Moffat,[8]
Slavek M. Rucinski,[9] and Werner W. Weiss[10]
Received 2006 October 9; accepted 2006 December 5

ABSTRACT

We have made a comprehensive transit search for exoplanets down to about 2 Earth radii in the HD 209458 system, based on nearly uninterrupted broadband optical photometry obtained with the *MOST* (*Microvariability and Oscillations of Stars*) satellite, spanning 14 days in 2004 and 44 days in 2005. We have searched these data for limb-darkened transits at periods other than that of the known giant planet, from about 0.5 days to 2 weeks. Monte Carlo statistical tests of the data with synthetic transits inserted allow us to rule out additional close-in exoplanets with sizes ranging from about 0.20–0.36 R_J (Jupiter radii), or 2.2–4.0 $R_\oplus$ (Earth radii) on orbits whose planes are near that of HD 209458b. These null results constrain theories that invoke lower mass planets in orbits similar to HD 209458b to explain its anomalously large radius, and those that predict "hot Earths" due to the inward migration of HD 209458b.

Subject headings: methods: data analysis — planetary systems

1. INTRODUCTION

Since the discovery of the first exoplanet around a Sun-like star, 51 Pegasi b (Mayor & Queloz 1995), over 200 other exoplanets have been discovered to date (Schneider[11]). Of these, a significant number have been "hot Jupiters," gas giant planets orbiting extremely near their parent stars. With the launch of the *MOST* (*Microvariability and Oscillations of Stars*) satellite (Walker et al. 2003; Matthews et al. 2004) in 2003 and the upcoming launches of the *COROT* (Baglin 2003; Barge et al. 2005) and *Kepler* (Borucki et al. 2004; Basri et al. 2005) space missions, the age of transit searches with continuous space-based photometry is now upon us. These new observatories signal that the discovery of an Earth-sized planet orbiting a Sun-like star is a prospect that can now be seriously anticipated.

The first transits of an exoplanet were observed in the system HD 209458, whose planet was discovered from radial velocity measurements by Mazeh et al. (2000). The transits were detected by Charbonneau et al. (2000) and Henry et al. (2000). The discovery of this transiting planet has led to concentrated studies of the system and hence improved knowledge of the star's characteristics (e.g., Wittenmyer et al. 2005; Mandel & Agol 2002; Knutson et al. 2007), which is critical for the determination of the radius and other properties of the known exoplanet and any additional transiting exoplanets found orbiting HD 209458. HD 209458 is a G0 V, $V = 7.65$ star (Laughlin et al. 2005) with effective temperature $T_{\rm eff} = 6000 \pm 50$ K, luminosity $L = 1.61\ L_\odot$ (Mazeh et al. 2000), mass $M = 1.10 \pm 0.07\ M_\odot$, and radius $R = 1.13 \pm 0.02\ R_\odot$ (Knutson et al. 2007).

There are theoretical reasons to expect smaller exoplanets in close orbits around HD 209458. The anomalously large size of the known exoplanet (Laughlin et al. 2005) has led to suggestions that the planet may be "puffed up" due to tidal heating involving the interaction of a second planet (Laughlin et al. 2005; Bodenheimer et al. 2001, 2003) in a resonant orbit with HD 209458b. Zhou et al. (2005) and Raymond et al. (2006) predict that the inward migration of hot Jupiter planets will lead to Earth-mass and super-Earth-mass planets in close orbits to their parent stars in systems such as HD 209458.

Detection of exoplanets around other stars via transit measurements is a field of increasing importance. Ground-based wide-field photometric surveys, such as the Transatlantic Exoplanet Survey (TrES; Alonso et al. 2004), Hungarian Automated Telescope (HAT; Bakos et al. 2002), Optical Gravitational Lensing Experiment (OGLE; Udalski et al. 2002), and SuperWASP (Street et al. 2004), are simultaneously monitoring thousands of nearby bright stars for evidence of transits. The discoveries of TrES-1 (Alonso et al. 2004), XO-1b (McCullough et al. 2006), TrES-2 (O'Donovan et al. 2006), and HAT-P-1b (Bakos et al. 2007) have illustrated the feasibility of discovering extrasolar planets via the transit method. Other ground-based surveys have focused primarily on globular and open clusters and have returned a series of null results (Weldrake et al. 2005; Hidas et al. 2005; Hood et al. 2005; von Braun et al. 2005; Burke et al. 2006; Mochejska et al. 2006). Space-based *Hubble Space Telescope* (*HST*) results returned a null result in the globular cluster 47 Tucanae (Gilliland et al. 2000), while more recently Sahu et al. (2006) detected 16 transiting planet candidates near the Galactic bulge.

[1] Based on data from the *MOST* satellite, a Canadian Space Agency mission, jointly operated by Dynacon, Inc., the University of Toronto Institute of Aerospace Studies, and the University of British Columbia, with the assistance of the University of Vienna.

[2] Department of Physics and Astronomy, University of British Columbia, Vancouver, BC, Canada; croll@astro.utoronto.ca, matthews@phas.ubc.ca, rowe@phas.ubc.ca, kuschnig@phas.ubc.ca, gladman@phas.ubc.ca, ccameron@phas.ubc.ca.

[3] Sumus Technology Limited; arwalker@sumusltd.com.

[4] Harvard-Smithsonian Center for Astrophysics, Cambridge, MA; sasselov@cfa.harvard.edu.

[5] 1234 Hewlett Place, Victoria, BC V8S 4P7, Canada; gordonwa@uvic.ca.

[6] University of California Observatories, Lick Observatory, University of California, Santa Cruz, CA; lin@ucolick.org.

[7] Department of Astronomy and Physics, St. Mary's University, Halifax, NS, Canada; guenther@ap.stmarys.ca.

[8] Observatoire du mont Mégantic, Département de physique, Université de Montréal, Montréal, QC, Canada; moffat@astro.umontreal.ca.

[9] Department of Astronomy and Astrophysics, David Dunlap Observatory, University of Toronto, Richmond Hill, ON, Canada; rucinski@astro.utoronto.ca.

[10] Institut für Astronomie, Universität Wien, Vienna, Austria; weiss@astro.univie.ac.at.

[11] J. Schneider, 2006, available at http://exoplanet.eu.

All ground-based transit searches are inherently limited by time sampling: the day-night cycle, weather, and sometimes observing-time allocation. In addition, their photometric precision means they are sensitive to only planets similar in scale to our giant planets. Space-based transit searches from satellites in inclined equatorial orbits (such as *HST*) also have limited time sampling. However, space-based transit surveys from platforms with large continuous viewing zones (CVZs) on the sky offer the potent combination of excellent extended-time coverage and high photometric precision.

In this paper, we describe such a search for transits in the HD 209458 system with the *MOST* satellite, with nearly continuous time coverage over two epochs spanning 2 and 6 weeks in 2004 and 2005, respectively. The methods refined and developed here to take advantage of this precise, high–duty-cycle photometry allow us to reliably detect transits as shallow as $\sim$0.5 mmag, corresponding to an exoplanet as small as about 0.2 R_J, or 2 $R_\oplus$. These methods are also applicable to other space-based transit searches, such as future searches with *MOST*, as well as those planned with the *COROT* and *Kepler* space missions.

In § 2 the *MOST* photometry of HD 209458 is described. The transit search technique is discussed in § 3. The Monte Carlo statistics used to estimate the sensitivity of the transit search are specified in § 4. The transit search routine is applied to the *MOST* HD 209458 data set in § 5, and the results are presented in § 6, including a discussion of the impact of these results on theories relating to other putative exoplanets in the system, and the characteristics of the known exoplanet HD 209458b.

2. *MOST* PHOTOMETRY OF HD 209458

The *MOST* satellite was launched on 2003 June 30, and its initial mission is described by Walker et al. (2003) and Matthews et al. (2004). A 15/17.3 cm Rumak-Maksutov telescope feeds two CCDs, one originally dedicated to tracking and the other to science, through a single, custom, broadband filter (350–700 nm). *MOST* was placed in an 820 km circular Sun-synchronous polar orbit with a period of 101.413 minutes. From this vantage point, *MOST* can monitor stars in a continuous viewing zone (covering a declination range $+36^\circ \leq \delta \leq -18^\circ$) within which stars can be monitored without interruption for up to 8 weeks. Photometry of very bright stars ($V \leq 6$) is obtained in Fabry Imaging mode, in which a Fabry microlens projects an extended image of the telescope pupil illuminated by the target starlight to achieve the highest precision (see Matthews et al. 2004). Fainter stars (down to about $V \sim 12$) can be observed in Direct Imaging mode, in which defocused images of stars are monitored in science CCD subrasters (see Rowe et al. 2006).

MOST observed HD 209458 in Direct Imaging mode over two separate epochs: for 14 days during 2004 August 14–30 (Rowe et al. 2006) and 44 days during 2005 August 2–September 15 (J. F. Rowe et al. 2007, in preparation). The first run was a trial, and testing of new onboard software led to several data interruptions, reducing the overall duty cycle of the raw photometry to about 85%. The second run returned data without significant interruptions, achieving an overall duty cycle of the raw photometry of 97%. The exposure time of the observations was 1.52 s, and the sampling rate was 10.0 s for both epochs of data. Approximately 112,000 and 361,000 individual observations were taken in the 2004 and 2005 epochs, respectively.

The reduction of the raw photometry downloaded from the satellite (and converted into FITS files) for both epochs was performed by J. F. R. The reduction is similar to that applied to ground-based CCD photometry but is nondifferential and incorporates both aperture and PSF (point-spread function) fitting. It corrects for cosmic-ray hits (especially frequent during satellite passages through the South Atlantic Anomaly [SAA]), the varying background due to scattered earthshine modulated at the satellite orbital period, and flat-fielding effects. Those data reduction techniques used are fully described in Rowe et al. (2006; J. F. Rowe et al. 2007, in preparation).

2.1. *Additional Filtering and Selection of the Data*

For this transit search, additional filtering and selection of the photometry was done to optimize the data for the application of Monte Carlo statistics. The filtering is an automated part of the transit search routine, and is thus briefly summarized in § 3.1. This filtering step is described in detail here.

Data obtained during passages through the SAA are conservatively excised from the light curve, due to the increased photometric scatter during those *MOST* orbital phases, without reducing seriously the phase coverage of the exoplanetary periods searched. The transits of the known giant planet HD 209458b are removed at the orbital period $P = 3.52474859$ days determined by Knutson et al. (2007). Because of the modulation of stray earthshine with *MOST*'s 101.4 minute orbital period, the data were phased to that period, and segments showing the most noticeable effects from stray light were also removed. The coverage in phase per 101.4 minute *MOST* orbit following this cut was 63% and 58% for the 2004 and 2005 epochs, respectively. The stray light background can also be modulated at a period of 1 day and its first harmonic (due to the Sun-synchronous nature of the *MOST* satellite orbit), so sinusoidal fits with periods within 1% of 1 and 0.5 days were subtracted from the data. After these cuts, any remaining outliers greater than 6 σ were excised. This sigma cut removed very few data points, as few points were such extreme outliers. The magnitude of the injected transits (§ 4) was always at a level much less than this sigma cut. The data were also median subtracted, for reasons outlined in § 3.5. The automatic filtering and selection step removed 45% of the original data (mostly due to the SAA and stray light corrections). The rms of the data following this additional filtering and selection step is 0.0035 mag.

The resulting HD 209458 light curves are plotted unbinned, and binned in 30 minute intervals in Figure 1. These filtered data (and the original reduced data) can be downloaded from the *MOST* Public Data Archive.[12]

3. TRANSIT SEARCH ALGORITHM

Our transit search routine has been developed and refined to take specific advantage of the unique time coverage of the *MOST* data. For HD 209458 in particular, it is designed to make use of the well-determined stellar and exoplanetary orbital parameters of the system. The search is intended to run automatically without user intervention to facilitate the generation of Monte Carlo statistics of the detection thresholds and their corresponding significances.

The entire routine (described in the following subsections) includes an automatic filtering and selection step (§ 3.1); a transit search algorithm, adapted from the EEBLS (Edge Effect Box-fitting Least Squares) algorithm of Kovács[13] sensitive to box-shaped transits (§ 3.2); selection criteria, to narrow the EEBLS candidates to a select few that can be tested for astrophysical plausibility (§ 3.3); transit model fitting, to identify realistic

[12] Available at: http://www.astro.ubc.ca/MOST.

[13] G. Kovács, 2003, available at http://www.konkoly.hu/staff/kovacs/index.html.

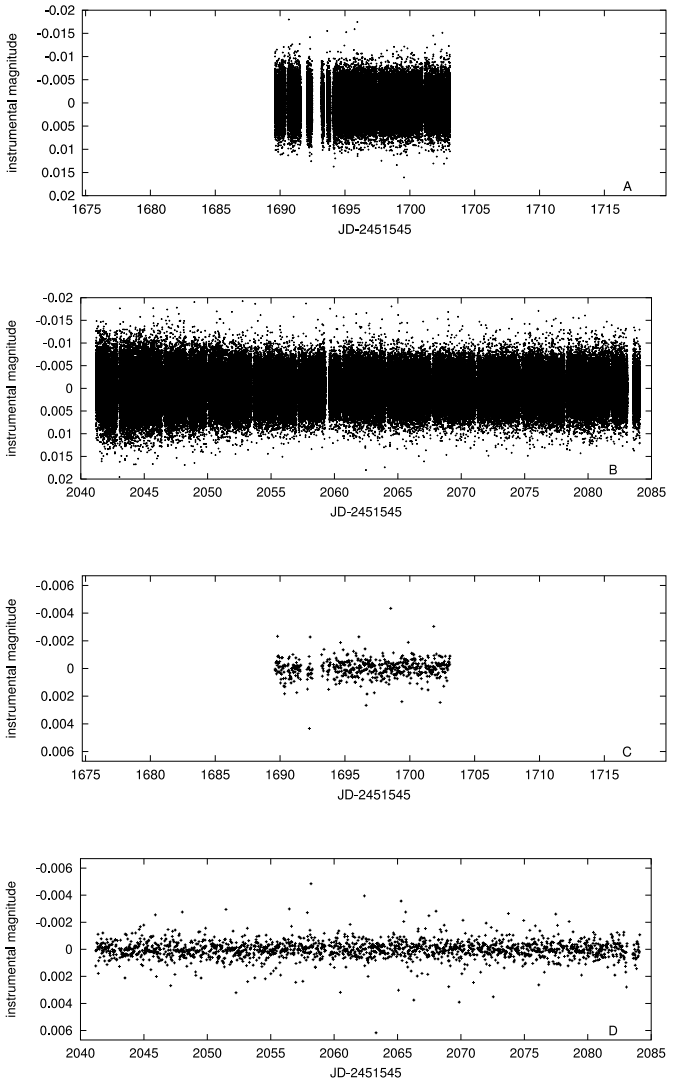

FIG. 1.—(*a*) 2004 and (*b*) 2005 HD 209458 *MOST* data sets following the initial reduction and the automatic filtering step. The same data are shown binned in 30 minute intervals at a different vertical scale for (*c*) 2004 and (*d*) 2005.

limb-darkened transit candidates for exoplanets of various radii, orbital periods, and inclination angles (§ 3.4); and finally detection criteria, to differentiate between likely transiting candidates and false positives (§ 3.5). This automated search routine can also be applied to other transit search experiments in which the characteristics of the target stars are well known or inferred.

3.1. *Automated Filtering and Selection Scheme*

The initial reduction scheme of J. F. R., as described in § 2, is almost entirely independent of the magnitude of an individual data point. Instead other indicators, such as the sky background level, are used to remove or adjust the data or the associated uncertainty of an individual data point. Therefore, inserting synthetic transits in the light curve after this initial reduction to produce Monte Carlo statistics is a valid procedure. To ensure proper application of those Monte Carlo statistics for this and other data sets, we incorporate an automated data-filtering and selection scheme in the transit search to filter out stray earthshine and to remove additional outliers and the dominant transits of the known exoplanet. This process was described in detail in § 2.1. It is briefly summarized here to ensure that it is obvious that this process is an automated part of the transit search routine applied to the Monte Carlo statistics to come. The thresholds and amplitudes used in this automatic filtering scheme have been optimized for their application to the *MOST* HD 209458 data; obviously these thresholds and amplitudes would have to be similarly optimized for their application to other *MOST* data sets.

3.2. *EEBLS Algorithm*

To search for transits in the HD 209458 system at periods other than that of the known exoplanet HD 209458b, we use a slight modification of the Box-fitting Least Squares (BLS) algorithm (Kovács et al. 2002), namely the Edge-Effect Box-fitting Least Squares (EEBLS) algorithm (Kovács). The EEBLS routine flags putative transit candidates by searching for box-shaped transits in a light curve. The signal strength of a putative transit is indicated by the signal residue (SR), as defined in Kovács et al. (2002). The SR is roughly equivalent to the χ^2 for a box-shaped transit, as indicated in the Appendix of Burke et al. (2006). The EEBLS routine returns the period, phase, and drop in magnitude of the supposed transit. The EEBLS algorithm was chosen because it has been used extensively in similar searches (e.g., Burke et al. 2006; Mochejska et al. 2006; Sahu et al. 2006) and quantitative comparisons indicate it is as good as others in the literature (Tingley 2003).

As is the case with all computational routines that must handle a large number of data and an extensive search-parameter grid, sufficient resolution must be balanced against computational duration. To decrease the latter, we employ even logarithmic period spacing of the search grid, as suggested by Burke et al. (2006). With even logarithmic period spacing, the subsequent period searched, P_2, is related to the previous, P_1, by $P_2 = P_1(1 + \eta)$, where $\eta \ll 1$. Although even frequency spacing was used in the original formulation of BLS by Kovács et al. (2002), even logarithmic period spacing retains high sensitivity to transits with both short and long orbital periods without increasing computational duration. Both even frequency and even logarithmic period spacing are valid with sufficient resolution. We chose the value $\eta = 0.000168$ to attain the especially fine period resolution needed to resolve putative transits occurring in the two epochs of *MOST* data separated by the near 1 yr gap.

In this work, we search the data set for periods greater than $P_{\rm min} = 0.5$ days and less than $P_{\rm max} = 14.7$ days. The maximum period limit is set by our requirement to observe at least three hypothetical transits of a putative planet in the longer 2005 run (44 days). The minimum period was set to be 0.5 days, likely below the astrophysically reasonable period of the orbit of a stable exoplanet in the HD 209458 system, as it would correspond to a semimajor axis less then $\sim$2.5 times the stellar radius.

The EEBLS routine was also modified to enhance its detection sensitivity. For each trial period, the EEBLS routine was changed to record the most significant boxcar dimming (transit) and boxcar brightening signals independently. The original formulation recorded the most significant boxcar event, regardless of whether it was a dimming or a brightening. This resulted in a modest decrease in sensitivity as the noise floor increased because the algorithm was automatically including brightening events that could not possibly be transits. This reformulation allows one to better differentiate possible transits from systematic brightening events.

In addition, the minimum and maximum fractional transit lengths, *Qmi* and *Qma*, respectively, that the EEBLS algorithm searches each trial period for were set to be variable, rather than constant as in the original formulation. The small-planet approximation of Mandel & Agol (2002), as discussed below, was used to determine the approximate maximum fractional transit length for each trial period, Qm_P. For this approximation, a planet with radius $R_p = 0.4\,R_{\rm J}$, and with inclination angle $i = 90^\circ$ was used

TABLE 1
EEBLS Input Parameters

Variable	Definition	Value
Np	Number of period points searched	20000
η	Logarithmic period step	0.000168
$P_{\min}$	Minimum period submitted to EEBLS algorithm	0.5 days
$P_{\max}$	Maximum period submitted to EEBLS algorithm	14.7 days
Qmi	Minimum fractional transit length to be tested	$0.75Qm_P$
Qma	Maximum fractional transit length to be tested	$1.1Qm_P$
Nb	Number of bins in the folded time series at each test period	$20.0/Qmi$

to determine this maximum fractional transit length. This change is significant because the difference in the maximum fractional transit length falls from nearly $Qm_P \approx 0.13$ at the minimum period of 0.5 days to $Qm_P \approx 0.015$ at the maximum period of 14.7 days. This change allows one to thus use the known characteristics of the star that is investigated to precisely tailor the EEBLS search routine. *Qmi* and *Qma* were set significantly lower and slightly larger, respectively, than this maximum fractional transit length for each period; that is, *Qmi* was set as 0.75 times as large, and *Qma* was set as 1.1 times as large as the maximum fractional transit length for each period. These values of 0.75 and 1.1 times as large as the maximum fractional transit length were chosen because they span the parameter range of interest from a large edge-on planet to a small grazing planet.

The final change that was implemented was to set a variable number of bins in the folded time series at each test period, *Nb*, rather than the constant number as in the original formulation. This was again related to the fact that the maximum fractional transit length varies significantly from the minimum to maximum period investigated in this formulation. The decision was made to ensure that there was a constant number of bins in the folded time series during the in-transit component for the smallest fractional transit length, *Qmi*, for each trial period. This constant number of bins was set arbitrarily at 20, as it was believed this was large enough to properly determine the phase of a putative transiting planet. That is, for each trial period *Nb* was set as $20.0/Qmi$. *Nb* thus varied from as low as $\approx$200 for the minimum period of 0.5 days to as high as $\approx$1570 for the maximum period of 14.7 days. These changes not only increase the sensitivity of the algorithm to long-period events, but also marginally decrease the computational duration of the EEBLS algorithm. The EEBLS input parameters are summarized in Table 1.[14]

3.3. *Transit Selection Criteria*

The EEBLS algorithm returns the SR versus period for each of the *Np* periods investigated. Selection criteria have been developed to pick the most likely genuine transit candidates. These selection criteria are described here. Of all the periods, only those that are strong local maxima in SR versus period are flagged for further investigation. A strong local maximum is defined as one for which SR is greater than the $0.003nP$ neighboring period points in both directions. Of the strong local maxima, the candidates with the two highest SR signals are chosen for further analysis. As we often noted that simply picking the top SR values biases one's selection against short-period planets of small radius, a second selection criterion was implemented to ensure adequate sensitivity to short-period events ($\sim 0.5 < P <\sim 4.0$). The top two candidates with SR values 1.8 times greater than the SR noise floor were also selected for additional study. The SR noise floor is defined as the mean of the SR values for all period points within $0.2nP$ of the period of interest. These two selection criteria narrowed the list of prospective candidates to a maximum of four of the most likely transit candidates. Extensive statistical tests (described in § 4) both verified and refined the above criteria.

The EEBLS SR spectrum for the *MOST* HD 209458 2004 and 2005 light curves is shown in Figure 2; the candidates that passed the selection criteria for these light curves are also identified in Figure 2.

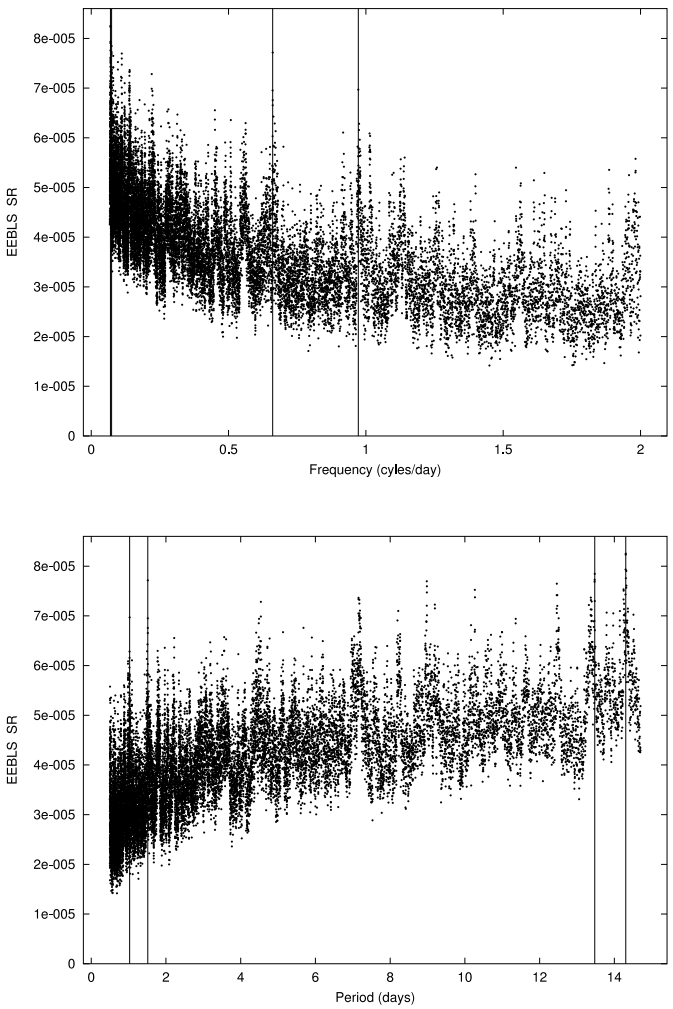

Fig. 2.—EEBLS spectrum of the total *MOST* HD 209458 data set, plotted in frequency (*top*) and period (*bottom*). The four candidates that passed the transit selection criteria as discussed in § 3.3 are shown by the solid vertical lines. In the frequency plot, the lines marking the two candidates with the lowest frequencies appear as one.

[14] The modified version of this algorithm in C is available at www.astro.ubc.ca/MOST/EEBLSmodified.cpp.

We also optimize the determination of the exact period, P, and phase, ϕ, for these candidates by rerunning the EEBLS algorithm with greater period, and then phase resolution, in the immediate period space of the candidate event. First, we run the EEBLS algorithm with greater period resolution from a minimum to maximum period of 4 period points less to 4 period points greater, respectively, than the best-fit period. An order of magnitude more period points are then used (100 points) to more accurately determine the period at which the greatest SR signal is returned. The period that returns the highest EEBLS SR is then investigated with the EEBLS algorithm at this one specific period with 5 times as many phase points as previously. These two steps are of negligible computational duration, but considerably increase the accuracy with which the period and phase are returned.

3.4. *Realistic Transit Fitting*

Since the discovery of the giant exoplanet HD 209458b, there has been intensive study of the star HD 209458, such that its basic characteristics are now well known (Wittenmyer et al. 2005; Knutson et al. 2007). This allows for considerable improvement in the shape, duration, and depth of the transit model as opposed to the original box-shaped transit used in the EEBLS routine. Specifically, we search for realistic limb-darkened transits of a specific period, P, planet radius, R_p, orbital inclination angle, i, and phase of transit, ϕ. Our model uses the small-planet approximation of Mandel & Agol (2002) to set the shape, length, and depth of the transit. The small-planet approximation of Mandel & Agol (2002) is valid for $R_P/R_* < 0.1$, and thus should be valid for HD 209458 for all transiting planets below $R_P \approx 1.1\ R_J$. We have only searched for transiting planets whose orbits are circular ($e = 0$); the impact of eccentricity is discussed in § 4. The HD 209458 system parameters used for our analysis are given in Table 2.

The transit candidates are then fitted by our limb-darkened transit model. For the period P returned by the EEBLS algorithm, two inclination angles i are investigated. One inclination angle is edge-on ($i = 90^\circ$), while the other is evenly spaced between the minimum inclination that would produce a transit ($\cos i \sim R_*/a$, where a is the semimajor axis), and an edge-on ($i = 90^\circ$) orbit. For short-period events, where the minimum inclination that would produce a transit is below 78°, the minimum inclination for the initial guess is arbitrarily set to 78°, as it was found that this increased the detection efficiency. For example, a period of approximately 4 days will have a minimum inclination angle of 84°, and thus the two guesses will be 87° and 90°, respectively. For these inclination angles, the planet radius R_p, phase ϕ, and inclination i, of a putative transit are fit through a Marquardt-Levenberg nonlinear least-squares algorithm (Marquardt 1963; Levenberg 1944; Press et al. 1992). Different starting values for the orbital inclination are used, since it was found through Monte Carlo analysis of simulated transits (§ 4) that this improved the efficiency in returning the correct value of i. The initial guesses in radius, R_p, and phase, ϕ, given to the Marquardt-Levenberg algorithm are the characteristics returned by the EEBLS routine, where the dimming in brightness is translated into the size of a hypothetical edge-on planet using the known stellar radius. Limits were placed on the range of parameters that the Marquardt-Levenberg algorithm could explore, away from the starting points returned by the EEBLS algorithm, to ensure that the fit would remain in the parameter space that was flagged as significant by the EEBLS algorithm. These were $\Delta R_p \approx 0.10$, $\arccos(R_*/a) \leq i \leq 90.0^\circ$, and $\Delta\phi \approx 0.05$. Fitting for the period as well using the Marquardt-Levenberg nonlinear least-squares algorithm was not attempted here, as the period optimization discussed above was deemed sufficient. The values of R_p, i, and ϕ that produce the minimum χ^2 value are recorded as the best transit candidate for that period.

TABLE 2
System Parameters

Variable	Definition	Value
R_*	Stellar radius	1.125 $R_\odot$[a]
M_*	Stellar mass	1.101 $M_\odot$[a]
c_1	Nonlinear limb-darkening parameter 1	0.410769[b]
c_2	Nonlinear limb-darkening parameter 2	−0.108909[b]
c_3	Nonlinear limb-darkening parameter 3	0.904020[b]
c_4	Nonlinear limb-darkening parameter 4	−0.437364[b]

[a] Parameters obtained from Knutson et al. (2007).
[b] These limb-darkening parameters are fully described in Mandel & Agol (2002) and obtained from Knutson et al. (2007) and J. F. Rowe et al. (2007, in preparation).

An attempt was made to bypass the EEBLS algorithm altogether and solely use the above fitting method to search for realistic limb-darkened transits in the *MOST* HD 209458 data. However, this approach proved very computationally intensive, and so we adopted and recommend the compromise described above, which achieves sufficient accuracy without significant increase in computational duration.

3.5. *Transit Detection Criteria*

We have developed quantitative criteria to differentiate bonafide transiting planet candidates from false positive detections without the need for detailed visual inspections of every set of candidate events in the light curve. We compare each modeled transit candidate to an antitransit (brightening) model and a constant brightness model. The latter assumes a star of constant magnitude, given by the mean of the light curve. The transit model consists of an out-of-transit component and an in-transit component (modeled as described in § 3.4). The out-of-transit component has a constant brightness level given by the median of the light curve; the median was chosen, as opposed to the mean, because it should remain relatively unchanged regardless of whether one or more other transiting planets are present in the HD 209458 system. During transit a realistic limb-darkened transit of a spherical planet is used, with parameters R_p, i, and ϕ, as returned by the fit described in § 3.4 and the small-planet approximation of Mandel & Agol (2002).

The statistic that has been used to quantify the improvement of the transit model over the constant flux model is $\Delta\chi^2\%$, the percentage improvement in χ^2 of the transit model (χ^2_T) over the constant flux model (χ^2_C). That is, $\Delta\chi^2\% = 100(\chi^2_C - \chi^2_T)/\chi^2_C$. The antitransit model is identical to the transit model, except that the transit causes brightening as opposed to dimming. The best-fit antitransit model was determined through the identical method, as outlined in §§ 3.2–3.4. Simultaneously determining the best-fit transit and antitransit model results in a minor increase in computational duration, but this is a justified sacrifice, as it provides an independent method for determining the detection sensitivity. In a similar fashion, the improvement of the antitransit model ($\chi^2_{\rm AT}$) over the constant-brightness model is given by $\Delta\chi^2_-\% = 100(\chi^2_C - \chi^2_{\rm AT})/\chi^2_C$. The quantitative detection criteria were motivated by Burke et al. (2006) and have been refined through the Monte Carlo tests described in § 4.

A believable transit was defined as one that satisfied the following criteria:

1. Of the transits selected by the selection criteria (§ 3.3) the transit of interest showed the greatest improvement in $\Delta\chi^2\%$.

2. The ratio between the improvement of the transit model over the constant-brightness model versus the antitransit over the constant-brightness model is at least 1.01 ($\Delta\chi^2\%/\Delta\chi^2_-\% \geq 1.01$).

3. The quantity f, as defined by Burke et al. (2006) and explained below, is less than 0.65 ($f < 0.65$).

The first criterion is intended to be conservative, as it helps to avoid identifying harmonics of the period of an obvious transit candidate. The second criterion was suggested by Burke et al. (2006) for a ground-based transit survey, and is primarily used as a threshold to differentiate astrophysically credible transit candidates from false positives. We use a much more sensitive value for the ratio ($\Delta\chi^2\%/\Delta\chi^2_-\% \geq 1.01$), due to the increased sensitivity of the *MOST* space-based photometry, as well as the results of the Monte Carlo tests of § 4. The level that has been chosen requires the best-fit transit to be only slightly more prominent than the best-fit antitransit candidate. It is important to note that the best-fit antitransit is not restricted to at the same period as the best-fit transit. The best-fit antitransit is determined in a completely analogous fashion to the best-fit transit, and thus the parameters of the best-fit transit and antitransit are often completely independent. The motivation for selecting this sensitive value of 1.01 was based on the experience gained from the Monte Carlo results, as it was the set at that level at which a transit could be reliably recovered from the data set without inducing significant numbers of false positives. The full explanation of how the value of $\Delta\chi^2\%/\Delta\chi^2_-\% \geq 1.01$ was derived is given in § 4. The rationale for this cut, as noted by Burke et al. (2006), is that in the case that the light curve shows periodic variability or significant brightening or dimming trends, a transit search will often assign considerable significance to these events, possibly resulting in false positive detections. Although this cut has primarily been designed for wide-field or open and globular cluster transit searches, where eliminating targets that show obvious sinusoidal variation is desirable, it is still applicable to the present search to account for possible variations and trends due to stray earthshine or intrinsic variability in the star HD 209458. It should also be noted that only improvements in the antitransit model, $\Delta\chi^2_-\%$ ($\Delta\chi^2_-\% > 0$), are accepted. This is because in the limit of extremely deep transits, on the order of those visible by eye such as those produced by HD 209458b, the antitransit statistics are forced to return worse values of $\Delta\chi^2_-\%$, as no significant brightening event is detected. This is because the median rather than the mean is used for the out-of-transit component of our transit model. This effect was not observed in the current application, or in the Monte Carlo tests, but it is a useful caveat for other transit searches.

The third criterion invokes the parameter f, which Burke et al. (2006) defines as $f = \chi^2_{k\text{th}}/\chi^2_{\text{total}}$. Here χ^2_k refers not to the typical χ^2, but rather to summing the following quantity for the kth transit: $\chi^2_{k\text{th}} = (m_i^2/\sigma_i^2)$, where m_i and σ_i are the magnitude and uncertainty, respectively, of the ith measurement during the kth transit. The criterion requiring $f < 0.65$ roughly corresponds to observing the transit at least one and a half times, assuming similar noise. This criterion is useful in eliminating long-period false positive events, as it ensures that the dimming behavior that caused the EEBLS routine to flag the event as highly significant is actually observed at least one and a half times. This cut is of only limited significance to our HD 209458 search, given the sensitivity, time span, and high duty cycle of the *MOST* photometry. However, it remains a safeguard for some long-period events in our current search and for future ground- and space-based searches.

Avoiding false positives is necessary so as to not place unjustifiably sensitive limits in the Monte Carlo statistics of § 4. These or similar criteria should be suitable for other ground- and space-based transiting exoplanet searches.

4. MONTE CARLO STATISTICS

To assess the sensitivity of the aforementioned search routine and the *MOST* data set to other transiting planets in the HD 209458 system, simulated transits for planets of various radii and orbital parameters were inserted into the *MOST* photometry and Monte Carlo statistics of the transit recovery rate were generated.

Realistic limb-darkened transits due to planets with various radii R_p, orbital phases ϕ, periods P, and inclinations i were inserted into the 2004 and 2005 *MOST* HD 209458 data. The small-planet approximation of Mandel & Agol (2002) was used. The differences between the more accurate nonlinear model of Mandel & Agol (2002) and the small-planet model approximation are negligible for the size of planets inserted in this data set, even for transits with short periods and thus semimajor axes only a few times the stellar radius. These modified data were then subjected to the analysis described above. Transits were inserted with logarithmic period spacing (as discussed in § 3.2), with $\eta_{\text{inp}} = 0.095$ in the period range 0.55 days $< P_{\text{inp}} <$ 14.5 days. In total, 37 period steps were used for the 90° and 88° inclination angle cases. For other inclination angles, transits were inserted with logarithmic period spacing until the period exceeded the maximum period, or semimajor axis, that would produce a transit, $a < (R_* + R_P)/\cos i$. For each trial period, simulated transits corresponding to nine different exoplanet radii were inserted, sampling the period-radius space of interest. For each period and radius, 110, 65, or 25 phases were inserted as summarized in Figures 4 and 6. For each of these points, the phase ϕ was generated randomly to be in the range $0 \leq \phi < 1$. Because a 2.4 GHz Pentium processor with 1 Gbyte of memory can perform the transit search algorithm on an individual MOST HD 209458 data set in ~10 minutes, exploration of the entire grid just mentioned for all inclinations involves $\simeq 10^5$ iterations and 2.0 CPU years. The calculation was performed on the LeVerrier Beowulf cluster in the Department of Physics and Astronomy at the University of British Columbia using 45 dual-CPU compute nodes.

An inserted transit was judged to be detected if the parameters ϕ and P returned by the transit search algorithm were sufficiently close to the input values, ϕ_{inp}, P_{inp}. The returned period had to satisfy the following criteria: $|P - P_{\text{inp}}| < 0.1$ days and $|P/P_{\text{inp}} - 1| < 1\%$. The limits of the criterion for ϕ were dependent on the orbital period, because as the period of the putative transiting planet decreases, the fractional transit length increases accordingly. Thus, the accuracy required in the determination of ϕ was relaxed for shorter periods. The criterion on ϕ is $|\phi - \phi_{\text{inp}}| < 0.09 - 0.0054(P_{\text{inp}} - 0.5 \text{ days})/\text{day}^{-1}$. Obvious multiples of the period of the inserted planet, up to 4 times the inserted period, P_{inp}, as well as half-period ($P \approx \frac{1}{2} P_{\text{inp}}$), and one-third period ($P \approx \frac{1}{3} P_{\text{inp}}$) solutions as returned by the transit search algorithm (§ 3) were also accepted, as it was found for a low percentage of cases that harmonics or subharmonics of the inserted trial period were flagged as the best candidates. For the 90° inclination angle the best candidates had a period double, triple, or quadruple the inserted period, approximately 1.0%, 0.5%, and 0.3%, respectively, of the total transit detections in the Monte Carlo analysis, while half and one-third period solutions accounted for 0.3% and 0.1% of the aforementioned total, respectively.

These Monte Carlo results were also used to determine the level above which a transit recovered from the data set could be

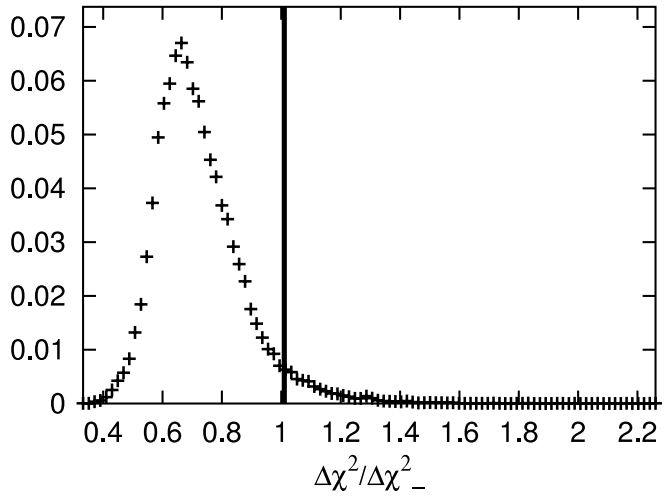

FIG. 3.—Histogram showing the improvement of the transit over the antitransit model ($\Delta\chi^2\%/\Delta\chi^2_-\%$) for all Monte Carlo candidates that are spurious (when the transit recovered by the transit routine is not the inserted transit). The threshold level for $\Delta\chi^2\%/\Delta\chi^2_-\%$, above which a transit can be considered significant, is determined via these statistics as it is set at a level, $\Delta\chi^2\%/\Delta\chi^2_-\% \approx 1.01$, that would rule out 95% of these spurious signals. The solid vertical line thus marks this threshold value.

considered significant. In deriving this value, one must be careful to closely balance the desire to use as low, and thus sensitive, a limit as possible with the necessity of limiting the number of false positive detections. Thus, to satisfy this rationale the following method has been used to determine this value of $\Delta\chi^2\%/\Delta\chi^2_-\%$ that will denote a believable transit. To determine a suitable value of the transit over the antitransit model ratio, $\Delta\chi^2\%/\Delta\chi^2_-\%$, all Monte Carlo cases where the candidate returned by the transit routine was not the candidate that was inserted were investigated. These events where the candidate returned by the routine was not the inserted transit will henceforth be referred to as spurious events.

By initially investigating the Monte Carlo statistics without the criterion that $\Delta\chi^2\%/\Delta\chi^2_-\% \geq 1.01$, we were able to investigate the maximum efficiency of the current transit routine. By comparing the efficiency of the Monte Carlo results with and without this threshold, one can quantitatively investigate the impact of this criterion. We restrict the investigation of these spurious signals to those that the routine has a reasonable chance of actually detecting. This area was determined to be the level above approximately the 25% contour of the Monte Carlo statistics when this threshold criterion was not used. Thus, for the generation of spurious signal statistics we only use those Monte Carlo cases with an input radius above the limit given here: $R_{P\mathrm{inp}} > [0.125 + (0.1/14.7)(P_{\mathrm{in}} - 0.5 \text{ days})/\text{days}]\, R_{\mathrm{J}}$.

A histogram of these spurious events versus $\Delta\chi^2\%/\Delta\chi^2_-\%$ for all inserted candidates above the radius threshold discussed can be seen in Figure 3. It was decided that a suitable level of $\Delta\chi^2\%/\Delta\chi^2_-\%$ would be one that ruled out 95% of these spurious events. Thus, the threshold level of $\Delta\chi^2\%/\Delta\chi^2_-\% \geq 1.01$ has a transit over antitransit ratio greater than 95% of these spurious signals. That is, if there is a transiting planet observable in the HD 209458 system, other than the known exoplanet HD 209458b, and the routine returns a putative transit that exceeds the threshold $\Delta\chi^2\%/\Delta\chi^2_-\% \approx 1.01$, one can be at least 95% certain that an actual transiting planet has been recovered, rather than a spurious signal. Since this measure has been calibrated to this *MOST* data set, the length of the time series has already been accounted for.

The fractions of times that the artificially inserted transits were recovered from the data for various radii, periods, and inclination angles are given in Figure 4. Also indicated in Figure 4 is the 68% contour limit that would be placed without the $\Delta\chi^2\%/\Delta\chi^2_-\% \geq 1.01$ criterion. The close agreement between the 68% contour with or without this criterion ($\Delta\chi^2\%/\Delta\chi^2_-\% \approx 1.01$) indicates that this criterion does not significantly impact the sensitivity of the Monte Carlo statistics generated, while providing a robust limit so as to avoid false positives and spurious detections.

We also explore the distribution of spurious signals across period-radii space. These values are displayed in Figure 5 and indicate that spurious signals are negligible (below 1%), other than in the intermediate areas where the routine has a small to moderate chance to correctly determine the inserted transit. In these intermediate areas in period-radius space, the inserted transit is small enough that correctly identifying the period, radius, and phase of the inserted transit using this routine is not guaranteed. However, the inserted transit is of sufficient magnitude to significantly impact the shape of the light-intensity curve and lead to spurious transit signals rising above the threshold, $\Delta\chi^2\%/\Delta\chi^2_-\% \geq 1.01$, for a small, but notable, percentage of cases. Accurately determining the frequency of true false positives—where there is not another transiting planet in the data set—as opposed to spurious signals is not attempted in this application, as it is difficult to produce a synthetic data set that accurately reproduces the systematics of the real data set. These systematics may be the result of imperfect removal of stray earthshine from the *MOST* data, or may, in fact, be intrinsic to the star.

We also investigated the performance of our routine at harmonics and subharmonics of the periods of the sinusoids that were removed from the data ($P = 1.0$ day and $P = 0.5$ days). Due to the fact that the fractional length of a transit is comparatively large for short periods of 0.5–1.0 days, it was found to be difficult to properly recover a transit signal near the harmonics and subharmonics of these periods for all cases. As expected and shown in Figure 6, the routine performs minimally worse near these values, as a portion of the transit signal is removed when the sinusoidal fit is removed in § 3.1. As can be seen in Figure 6, however, the period range demonstrating these drops in survey sensitivity is very narrow ($\Delta P/P \approx 2\%$), and the effect is very minor. Therefore very sensitive limits can still be set at these periods.

The harmonics and subharmonics of the period of the known planet HD 209458b, $P \approx 3.5247$ (Knutson et al. 2007), are also expected to show decreased sensitivity to transits due to the fact that the transits of the known planet were excised from the data. This reduction of sensitivity at these periods is unfortunate, considering that it is expected that low-mass planets show a preference for these resonant orbits (Thommes 2005; Zhou et al. 2005). The fractional length in phase that was removed at $P \approx 3.5247$ for the transit was 4.1% of the total. Thus, for the subharmonics of the known planet ($P \approx 7.05, 10.6, 14.1$ days), in approximately 4.1% of the cases the transits will coincide with the transits of the known planet, and thus the routine will be unable to recover the transiting planet because this data will have been completely removed. For these periods the 99% and 95% contours of Figure 4 would likely be seriously affected, although the 68% contour should only be slightly affected. For the harmonics of the orbital period of HD 209458b, the situation is better, since not all of the transit events would be removed from the data. For periods near the first harmonic ($P \approx 1.76$ days), every second occurrence of a transit will be lost in only 8.2% of the cases. For the second harmonic ($P \approx 1.17$ days), every third transit would be missed in 12.3% of the cases. For periods near these values the sensitivity limits can be

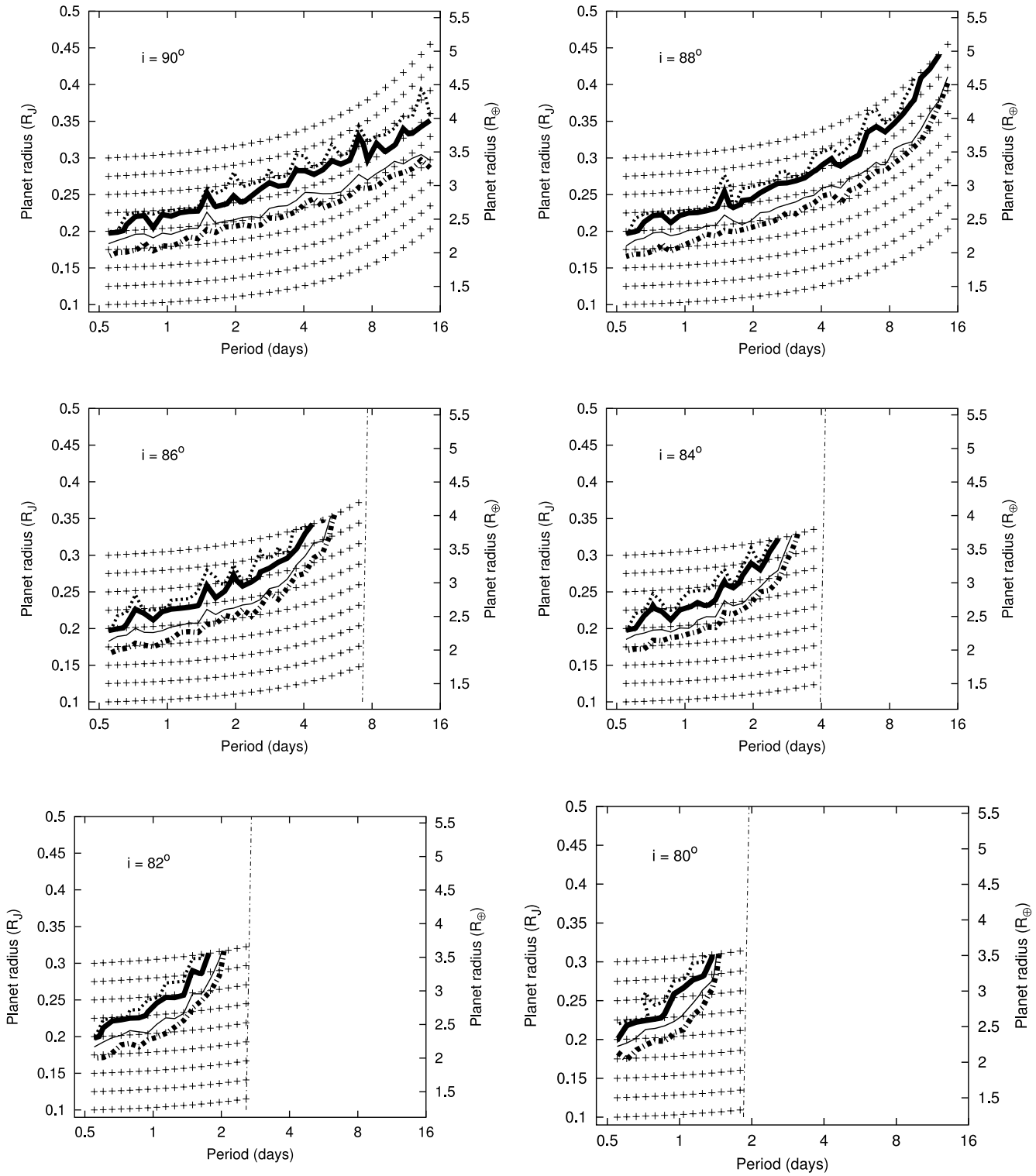

FIG. 4.—Confidence limits in transit detection as a function of planet radius and planetary orbital period, for different orbital inclinations, based on Monte Carlo statistics. The plus signs represent the radii and periods at which synthetic transits were inserted in the data. The dotted lines, thick solid lines, and thin solid lines represent the 99%, 95%, and 68% confidence contours, respectively. The thick dot-dashed line represents the 68% confidence contour if the criterion $\Delta\chi^2\%/\Delta\chi^2\% \geq 1.01$ was not used. The near-vertical dot-dashed line in the later panels indicates the maximum period that produces a transit for that given inclination angle. Note the logarithmic period scaling on the *x*-axis. There were 110 phases inserted for the 90° inclination angle case, while 65 phases were inserted for the other inclination angles.

expected to be only slightly degraded from those shown in Figure 4. Even for exact harmonics the routine's sensitivity should be only marginally worse than the limits quoted in Figure 4, as the remaining transits should allow the correct period (or a multiple of the period) to be recovered. These resonances have already been sensitively examined using the transit-timing technique on the known exoplanet HD 209458b (Agol & Steffen 2007; Miller-Ricci et al. 2006). Miller-Ricci et al. (2006) have applied this technique to the *MOST* photometry of HD 209458 and are able to rule out sub-Earth-mass planets near the inner harmonics of

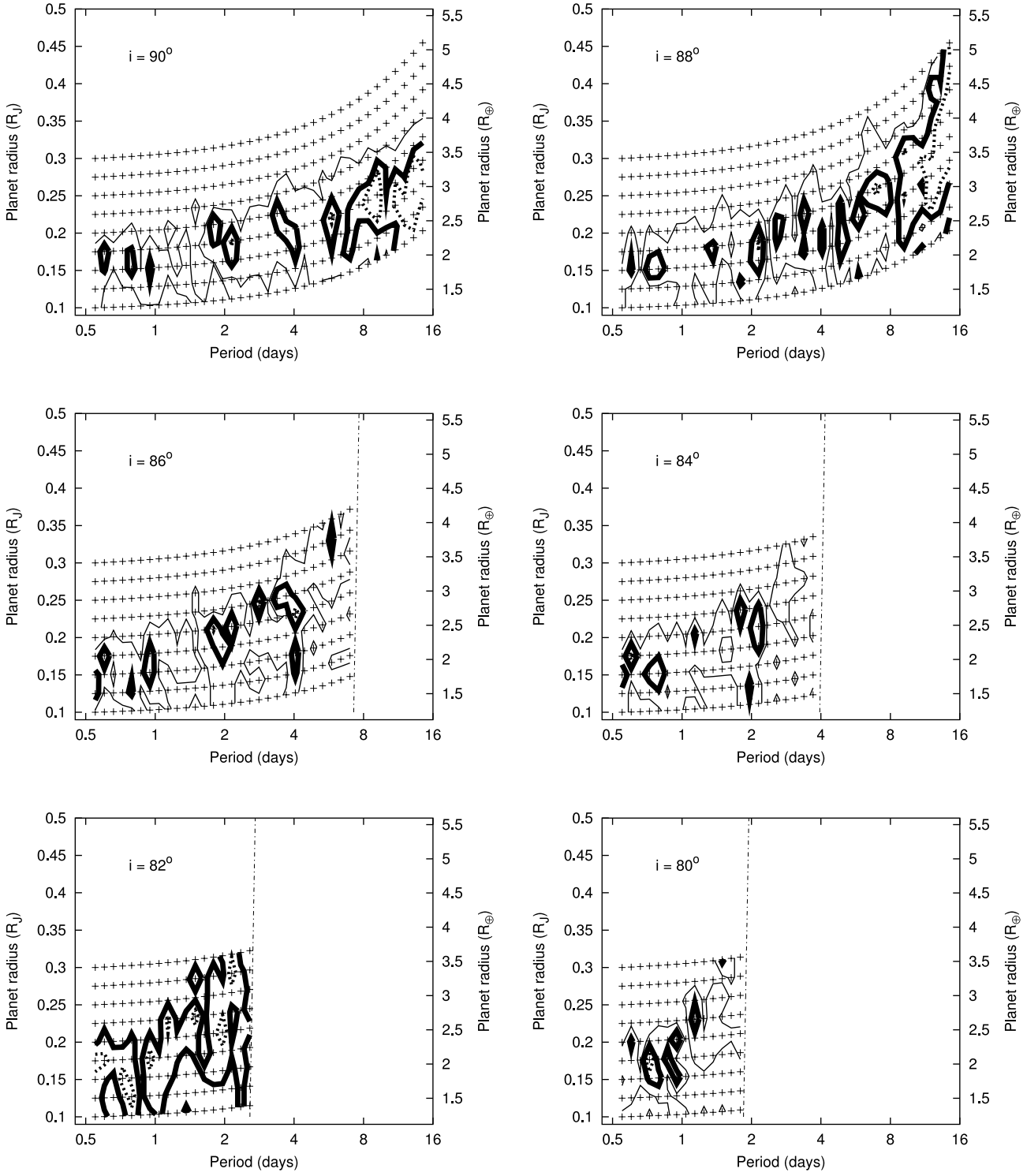

FIG. 5.—Likelihood of spurious transit detections returned by the Monte Carlo statistical analysis. The dotted lines, thick solid lines, and thin solid lines represent the 10%, 5%, and 1% spurious signal contours, respectively. The format of the figure is otherwise identical to Fig. 4. Note that the spurious signals occur in the intermediate regions of the period-radii space of interest, where it is not guaranteed that the correct transit will be recovered, but the inserted transit still causes significant deviations to the light curve.

HD 209458b and Earth- and super-Earth-mass planets near the outer subharmonics out to the 4:1 resonance.

The detection limits presented here are valid for circular orbits, but are largely applicable to orbits of other eccentricities. Eccentric orbits will increase, decrease, or have little effect on the fractional length of the transit, depending on whether the transit occurs near apastron, periastron, or in between, respectively. Obviously, the cases where the fractional transit length is increased will favorably affect the detection limits presented, while the opposite cases will adversely affect the detection limits. For low-eccentricity orbits this effect should be negligible, and thus the detection limits presented here should be largely applicable to these orbits. For non– edge-on

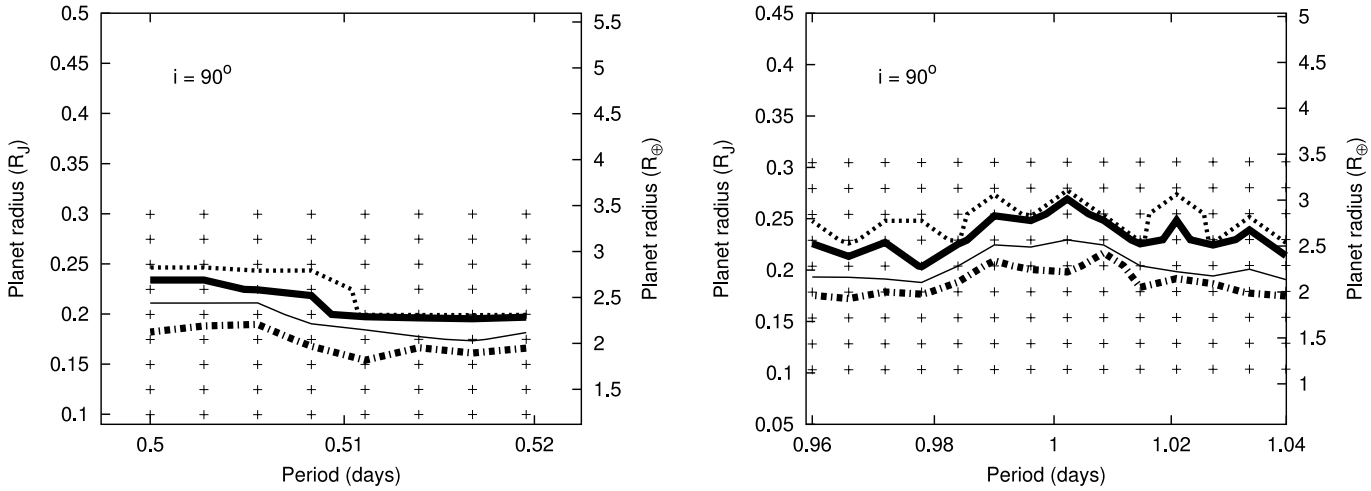

FIG. 6.—Transit search sensitivity near the periods of 0.5 days (*left*) and 1.0 days (*right*), where sinusoidal terms were filtered from the photometry. The format is the same as Fig. 4. There were 25 phases inserted for each period-radius point. As can be seen, the transit search sensitivity is only slightly adversely affected near these periods.

inclination angles, highly eccentric orbits will adversely affect the limits presented, as the planet will not transit the star along our line of sight for a greater fraction of the time. For edge-on, high-eccentricity orbits, the limits will likely be modestly adversely affected due to the cases where the transit occurs near periastron. Numerical simulations indicate that we would expect hot Earths or other exoplanets to have negligible eccentricities in the period range we are investigating (Raymond et al. 2006).

Thus, the search routine described above in § 3 should be able to detect planets with radii greater than the limits given in Figure 4. In the most optimistic case of an edge-on 90° inclination angle transit, for planets with periods of approximately a half a day to 2 weeks, this limit is approximately 0.20–0.36 R_J, or 2.2–4.0 $R_\oplus$, respectively, with 95% confidence. If one assumes a mean density of $\rho \approx 3000$ kg m^{-3}—a value averaging the various extrasolar super-Earth models discussed below—their respective masses would be 0.019 and 0.011 M_J, or 6 and 35 $M_\oplus$, respectively. If these putative planets were gaseous, and thus possible hot Neptune analogs ($\rho \approx 1600$ kg m^{-3}), a planet of $R_P = 4.0\,R_\oplus$ would result in a planetary mass of 19 $M_\oplus$. Thus the mass-period parameter space we have ruled out in this study, assuming these hypothetical mean densities, sets even tighter limits than those set by radial velocity observations of the system. Laughlin et al. (2005), for instance, ruled out other planets in the HD 209458 system with $M \sin i > 0.3\ M_J$ for $P < 100$ days. The planets we are thus able to rule out are one-fifteenth to one-third the mass of these radial velocity limits for edge-on transits. Full discussion of the mass of planets that have been ruled out in this study is given in § 6.1.

5. HD 209458 TRANSIT SEARCH

The *MOST* HD 209458 2004 and 2005 data sets were submitted to the analysis outlined in § 3. There were no transiting planet candidates that met the detection criteria as outlined in § 3.5. The details of the candidate with the greatest improvement in χ^2 are given in Table 3 and are shown in Figure 7. As this transiting candidate did not meet the detection criterion ($\Delta\chi^2\%/\Delta\chi^2_-\% \approx 0.893 < 1.01$), as outlined in § 3.5, we do not report it as a putative transiting candidate. This event, with a period of $P \approx 14.305$ days, has modest statistical significance, and thus we report that it is a possible, but unlikely, candidate. The characteristics of this planet are $P = 14.305$ days, $R_p = 0.261\ R_J$ (2.92 $R_\oplus$), and $i = 88.8°$. If this planet is a super Earth ($\rho \approx 3000$ kg m^{-3}) the mass of this putative planet would be approximately 13.6 $M_\oplus$ (0.043 M_J). A transit time combined with the supposed period is given in Table 3.

Although this event is at a period approximately 4 times that of the known planet, it is not expected that this event is related to an alias of the data due to the gaps associated with removing the transits of the known planet. The EEBLS algorithm is dissimilar to a Fourier transform in this regard, as gapped data of a certain period do not induce significant aliases at that period. Thus, removing the transits of the known planet should have fully removed all signal at the period, harmonics, and subharmonics of the known planet. This has been confirmed by limited numerical tests using data with the same time sampling as the data used in this application. A significant signal is not observed at harmonics or subharmonics of the known planet's orbital period statistically often in these tests. This putative signal at $P \approx 14.305$ days is therefore intrinsic to the data. Evidence for a transit at this period is marginal, but additional *MOST* photometry of the HD 209458 system should confirm or disprove its existence.

The most significant brightening event was one observed with a period of approximately $P \approx 8.96$ days. It is likely statistical in nature, and thus is not expected to be related to any specific astrophysical process.

As an additional sanity check this transit search method was applied to the current data set without the removal of the transits of the known planet, HD 209458b. As expected, the routine correctly uncovers the transit of HD 209458b to a high degree of accuracy. The actual parameters of HD 209458b (Knutson et al.

TABLE 3
TRANSIT CANDIDATE PARAMETERS

Parameter	Value
P	14.3053 days
R_p	0.261 R_J (2.92 $R_\oplus$)
i	88.8°
ϕ	0.871
Ephemeris minimum (JD − 2451545)	2051.4554
$\Delta\chi^2\%/\Delta\chi^2_-\%$	0.893
Mass (assuming $\rho \approx 3000$ kg m^{-3})	0.043 M_J (13.6 $M_\oplus$)

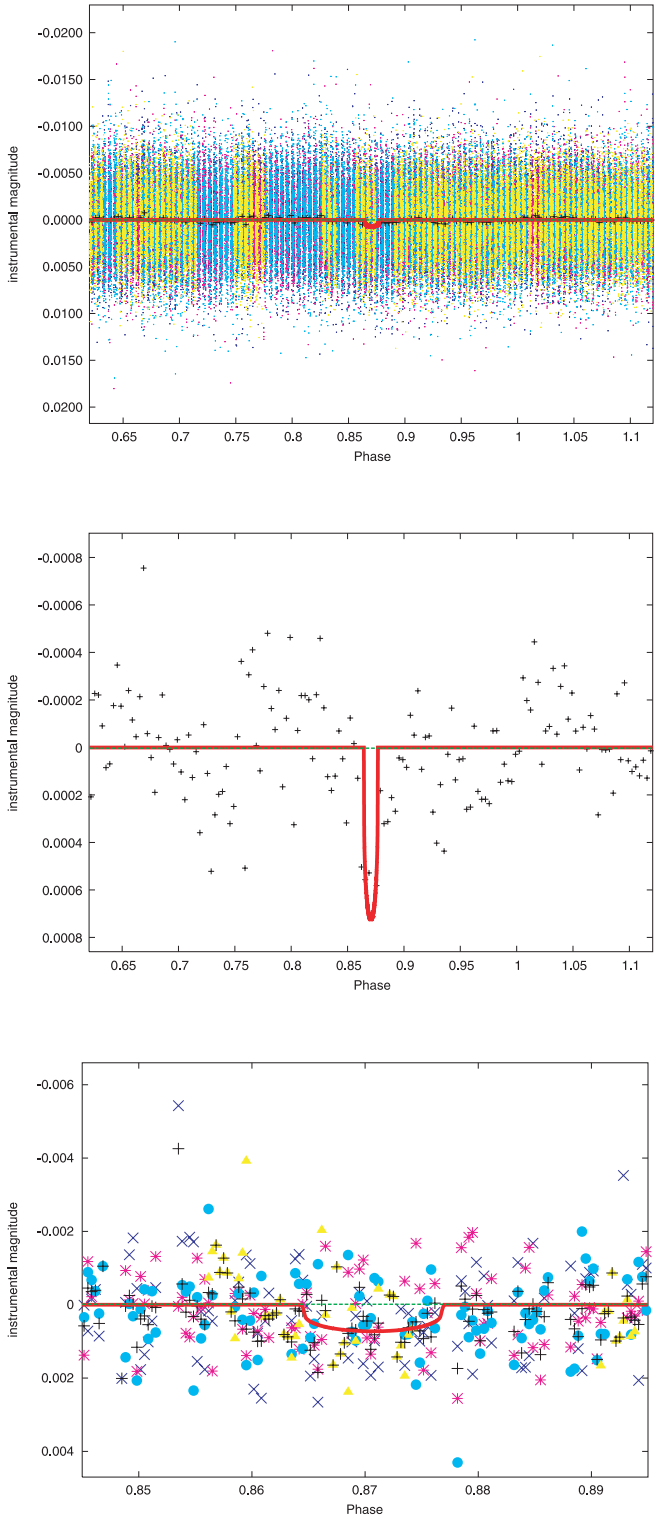

FIG. 7.—Best transit candidate, as identified by our analysis of *MOST*'s HD 209458 2004 and 2005 data sets, but with marginal significance. The red line represents the transit model, while the green dashed line represents the constant brightness model. *Top*: Data are unbinned in 2004 (*yellow points*) and the first (*cyan points*), second (*magenta points*), and third (*blue points*) putative transit in 2005, and binned (*black points*). *Middle*: Binned data only, at a different vertical scale. *Bottom*: Expanded portion of the phase diagram, with the binned data from the various transits given by the same colors as above. As this candidate failed the improvement in transit over antitransit criterion, $\Delta\chi^2\%/\Delta\chi^2_-\% \geq 1.01$, we report it as a possible but unlikely candidate. The period and radius of this putative planet would be approximately 14.3 days and 0.26 R_J (2.9 $R_\oplus$).

2007) were recovered within 0.0004% and 0.4% in period and phase, respectively, while the inclination angle and radius were recovered within 1.5°, and 0.02 R_J of the actual parameters.

6. DISCUSSION

MOST's 2004 and 2005 observations of HD 209458 have been searched for evidence of other exoplanets in the system. A transit search routine has been adapted to search for more realistic limb-darkened transits to take advantage of the precise, near-continuous photometry returned by *MOST* and the fact that the stellar characteristics of the star, HD 209458, are well established. Monte Carlo statistics were generated using this routine and indicate that this routine in combination with the aforementioned *MOST* data has placed unparalleled limits on the size of transiting bodies that have been ruled out in this system for a range of periods and inclination angles. In the most optimistic case of edge-on transits, planets with radii greater than 0.20 R_J (~2.2 $R_\oplus$) to 0.36 R_J (~4.0 $R_\oplus$) with periods from half a day to 2 weeks, respectively, have been ruled out with 95% confidence through this analysis. Specifically, we have been able to rule out transiting planets in this system with radii greater than those given in Figure 4. This work has constrained theories that invoke smaller exoplanets in the system to explain the anomalously large size of HD 209458b and those that predict "hot Earths" due to the inward migration of HD 209458b.

6.1. *Mass Constraints on Other Exoplanets in the System*

The above limits on the smallest planetary radii excluded by *MOST* for transiting planets allow some estimates on the type of planets that are being excluded. Planet radii change with time as the planet cools, so we make use of the fact that the age of the HD 209458 system is determined to be about 5 Gyr with an uncertainty of 1.0–1.5 Gyr (Cody & Sasselov 2002). This means that we can safely refer to cooling models similar to the planets in the solar system. One exception would be the consideration of possible planets in orbits smaller than that of HD 209458b, where tidal heating will lead to larger radii per given mass and composition.

Our radius limit of 2.2–4.0 $R_\oplus$ already places us in the realm of super-Earth and hot Neptune planets. The range of bulk compositions could encompass iron-rich cores [super-Mercuries, ~80% Fe or $Fe_{0.8}(FeS)_{0.2}$ core], super-Earths (less than 50% Fe core), water-rich super-Earths (more than ~10% H_2O), and water giants (hot Neptunes). Internal structure models for such planets have been published by Valencia et al. (2006, 2007). Hot Neptunes will have structures similar to Neptune (17.2 $M_\oplus$, 3.9 $R_\oplus$) and Uranus (14.4 $M_\oplus$, 4.0 $R_\oplus$). Planets with significant amounts of water should be referred to as "ice planets," because water ices VII and X would form at high pressures of a few GPa. At partial pressures exceeding ~100 MPa, ice planets are unlikely to evaporate (in 5 Gyr) in orbits larger than 0.1 AU (Valencia et al. 2007), while a pure H+He planet might (Yelle 2004).

In summary, our radius limit cannot exclude super-Mercuries of any Fe content, as their masses would have to exceed that of HD 209458b itself. It can exclude some super-Earths with masses larger than ~8 $M_\oplus$. It excludes water-rich super-Earths with masses larger than ~6 $M_\oplus$ for 50% water content and ~5.5 $M_\oplus$ for ice planets. The latter two types of planets will have radii that are very sensitive to stellar heating (hence their orbits) and tidal heating.

HD 209458 is a system that has experienced migration, and recent simulations for such planetary systems by Raymond et al. (2006) have confirmed previous expectations that water-rich Earths and super-Earths could often end up in orbits of 0.05–0.3 AU. Our transit search with *MOST* rules out super-Earths and hot Neptunes from 0.01 to 0.12 AU for HD 209458 for edge-on inclinations.

Planets with inclination angles substantially different than edge-on (see Fig. 4) cannot be ruled out with this photometry, except for very short periods. The radius limits presented here, combined with the mass limits from transit-timing analyses (Miller-Ricci et al. 2006; Agol & Steffen 2007), place very firm constraints on the size and masses of bodies that could still reside in close orbits to HD 209458. Reobservations of this system with *MOST* should be able to further reduce the size of planets that could remain undetected in this system, and further constrain theories invoking these planets in nearby orbits to HD 209458b. It will be very interesting to use *MOST* and obtain similar results for HD 189733 and HAT-P-1 and constrain such theoretical work.

6.2. *Radius and Mass Constraints on Trojans*

We can also place a limit on the size of Trojans that may be leading or trailing HD 209458b, assuming the Trojan consistently transits HD 209458 with an orbital inclination close to that of the known planet (87°). We use the definition of Trojans given by Ford & Gaudi (2006) of objects occupying the L4 or L5 Lagrangian points. Trojans lagging or leading HD 209458b with a radius above $R = 0.30\ R_J$ ($3.4\ R_\oplus$) should have been detected with this analysis with 95% confidence. The 99% confidence contour is only slightly larger, $R = 0.31\ R_J$ ($3.5\ R_\oplus$). If these putative planets were super-Earth analogs ($\rho \approx 3000$ kg m^{-3}) the corresponding mass limits would be $M = 21\ M_\oplus$ and $M = 23\ M_\oplus$ at 95% and 99% confidence, respectively, while for hot Neptune analogs ($\rho \approx 1600$ kg m^{-3}) the mass limits would be $M = 11\ M_\oplus$ and $M = 12\ M_\oplus$. Depending on the structure of planet that is assumed, these mass limits are comparable to or moderately worse than the $13\ M_\oplus$ 99.9% confidence limit of Ford & Gaudi (2006) for HD 209458. However, a detailed study using this *MOST* photometry of HD 209458 should be able to drastically improve this limit. It should be noted that Ford & Gaudi (2006) cast doubt on the hypothesis that a hypothetical Trojan will consistently transit HD 209458. They note that if the hypothetical Trojan has a vertical libration amplitude greater than approximately 9° it will not consistently transit HD 209458.

We thank the referee, Ron Gilliland, for useful comments that have improved this paper. We thank Sara Seager for useful discussions on exoplanetary mass models. The Natural Sciences and Engineering Research Council of Canada supports the research of D. B. G., J. M. M., A. F. J. M., J. F. R., S. M. R., G. A. H. W., and B. G. Additional support for A. F. J. M. comes from FCAR (Québec). R. K. and A. W. are supported by the Canadian Space Agency. W. W. W. is supported by the Austrian Space Agency and the Austrian Science Fund (P17580). The Canadian Foundation for Innovation provided funding for the LeVerrier Beowulf cluster.

REFERENCES

Agol, E., & Steffen, J. H. 2007, MNRAS, 374, 941
Alonso, R., et al. 2004, ApJ, 613, L153
Baglin, A. 2003, Adv. Space Res., 31, 345
Bakos, G. Á, Lázár, J., Papp, I., Sári, P., & Green, E. M. 2002, PASP, 114, 974
Bakos, G. Á., et al. 2007, ApJ, 656, 552
Barge, P., et al. (the COROT Team). 2005, in Conf. Ser. SF2A-2005, Semaine de l'Astrophysique Francaise, ed. F. Casoli et al. (Strasbourg: EdP-Sciences), 193
Basri, G., Borucki, W. J., & Koch, D. 2005, NewA Rev., 49, 478
Bodenheimer, P., Laughlin, G., & Lin, D. N. C. 2003, ApJ, 592, 555
Bodenheimer, P., Lin, D. N. C., & Mardling, R. A. 2001, ApJ, 548, 466
Borucki, W., et al. 2004, in Second Eddington Workshop: Stellar Structure and Habitable Planet Finding, ed. F. Favata, S. Aigrain, & A. Wilson (ESA SP-538; Noordwijk: ESA), 177
Burke, C. J., Gaudi, B. S., DePoy, D. L., & Pogge, R. W. 2006, AJ, 132, 210
Charbonneau, D., Brown, T. M., Latham, D. W., & Mayor, M. 2000, ApJ, 529, L45
Cody, A. M., & Sasselov, D. 2002, ApJ, 569, 451
Ford, E., & Gaudi, B. S. 2006, ApJ, 652, L137
Gilliland, R. L., et al. 2000, ApJ, 545, L47
Henry, G. W., Marcy, G. W., Butler, R. P., & Vogt, S. S. 2000, ApJ, 529, L41
Hidas, M. G., et al. 2005, MNRAS, 360, 703
Hood, B., et al. 2005, MNRAS, 360, 791
Knutson, H., Charbonneau, D., Noyes, R. W., Brown, T. M., & Gilliland, R. L. 2007, ApJ, 655, 564
Kovács, G., Zucker, S., & Mazeh, T. 2002, A&A, 391, 369
Laughlin, G., Marcy, G. W., Vogt, S. S., & Fischer, D. A. 2005, ApJ, 629, L121
Levenberg, K. 1944, Quart. Appl. Math. 2, 164
Mandel, K., & Agol, E. 2002, ApJ, 580, L171
Marquardt, D. W. 1963, SIAM J. Appl. Math. 11, 431
Matthews, J. M., Kusching, R., Guenther, D. B., Walker, G. A. H., Moffat, A. F. J., Rucinski, S. M., Sasselov, D., & Weiss, W. W. 2004, Nature, 430, 51
Mayor, M., & Queloz, D. 1995, Nature, 378, 355
Mazeh, T., et al. 2000, ApJ, 532, L55
McCullough, P. R., et al. 2006, ApJ, 648, 1228
Miller-Ricci, E., et al. 2006, ApJ, submitted
Mochejska, B. J., et al. 2006, AJ, 131, 1090
O'Donovan, F. T., et al. 2006, ApJ, 651, L61
Press, W. H., Teukolsky, S. A., Flannery, B., & Vetterling, W. T. 1992, Numerical Recipes in FORTRAN (2nd ed.; Cambridge: Cambridge Univ. Press)
Raymond, S., Mandell, A., & Sigurdsson, S. 2006, Science, 313, 1413
Rowe, J. F., et al. 2006, ApJ, 646, 1241
Sahu, K. C., et al. 2006, Nature, 443, 534
Street, R. A., et al. 2004, Astron. Nachr., 325, 565
Thommes, E. W. 2005, ApJ, 626, 1033
Tingley, B. 2003, A&A, 408, L5
Udalski, A., et al. 2002, Acta Astron., 52, 1
Valencia, D., O'Connell, R., & Sasselov, D. 2006, Icarus, 181, 545
Valencia, D., Sasselov, D. D., & O'Connell, R. J. 2007, ApJ, 656, 545
von Braun, K., Lee, B. L., Seager, S., Yee, H. K. C., Mallén-Ornelas, G., & Gladders, M. D. 2005, PASP, 117, 141
Walker, G. A. H., et al. 2003, PASP, 115, 1023
Weldrake, D. T. F., Sackett, P. D., Bridges, T. J., & Freeman, K. C. 2005, ApJ, 620, 1043
Wittenmyer, R. A., et al. 2005, ApJ, 632, 1157
Yelle, R. 2004, Icarus, 170, 167
Zhou, J. L., Aarseth, S. J., Lin, D. N. C., & Nagasawa, M. 2005, ApJ, 631, L85